Plant Physiology and Biochemistry 137 (2019) 75–83

Contents lists available at ScienceDirect

Plant Physiology and Biochemistry

journal homepage: www.elsevier.com/locate/plaphy

Research article

Genome-wide identification of genes involved in carbon fixation in *Saccharina japonica* and responses of putative C_4-related genes to bicarbonate concentration and light intensity

Zhanru Shao[a,b,c], Wenli Wang[d], Pengyan Zhang[a,e], Jianting Yao[a,b,c], Fahe Wang[d], Delin Duan[a,b,c,d,*]

[a] *CAS Key Laboratory of Experimental Marine Biology, Institute of Oceanology, Chinese Academy of Sciences, No.7 Nanhai Road, Qingdao, 266071, China*
[b] *Laboratory for Marine Biology and Biotechnology, Qingdao National Laboratory for Marine Science and Technology, No.1 Wenhai Road, Jimo, Qingdao, 266237, China*
[c] *Center for Ocean Mega-Science, Chinese Academy of Sciences, No.7 Nanhai Road, Qingdao, 266071, China*
[d] *State Key Laboratory of Bioactive Seaweed Substances, Qingdao Brightmoon Seaweed Group Co Ltd, No.777 Mingyue Road, Qingdao, 266400, China*
[e] *Yellow Sea Fisheries Research Institute, Chinese Academy of Fishery Sciences, No.106 Nanjing Road, Qingdao, 266071, China*

ARTICLE INFO

Keywords:
Carbon fixation
Environmental influences
Enzymatic activity
mRNA abundance
Saccharina japonica

ABSTRACT

Brown algae play a dominant role in the primary productivity of coastal ecosystems and may have an efficient carbon fixation. In this work, 56 genes involved in inorganic carbon fixation were identified from the *Saccharina japonica* genome. Sequence structure analysis of these genes showed the existence of corresponding function domains and active amino acid sites highly conserved with other stramenopile species. The predicted subcellular localizations showed that Calvin cycle-related enzymes predominantly reside in the plastid and that putative C_4-related enzymes are mainly distributed in the mitochondrion. We determined the transcriptional profiles and enzymatic activities of these C_4-related enzymes in response to the $KHCO_3$ concentrations and light intensities. Pyruvate orthophosphate dikinase (PPDK) presented the greatest response to low HCO_3^- concentrations and high light intensity. Phosphoenolpyruvate carboxykinase (PEPCK) was up-regulated at low HCO_3^- concentrations to compensate for ribulose-1,5-bisphosphate carboxylase/oxygenase (Rubisco) and might be the crucial decarboxylase in this kelp. We propose that *S. japonica* might possess a PPDK- and PEPCK-dependent C_4-like pathway that enables its rapid growth in natural coastal environments.

1. Introduction

Seaweeds are important marine photoautotrophs and play an important role in global primary production (Nellemann et al., 2009). Marine macroalgae mainly inhabit littoral zones and account for approximately 50% of the carbon fixation ($\sim$210–240 Tg C y^{-1}) in coastal ecosystems (Duarte et al., 2005), with important economic value as sources of '3rd generation biomass' (Xu et al., 2014).

Approximately 90% of dissolved inorganic carbon in seawater environments (pH 8.1–8.4) exists as bicarbonate ions (HCO_3^-) and the remainder as carbonate ions (CO_3^{2-}) and dissolved CO_2 (Skirrow, 1975; Doney et al., 2009). Macroalgae assimilate inorganic carbon via three mechanisms: free diffusion of CO_2 across cell membranes, conversion of extracellular HCO_3^- into CO_2 by a secreted carbonic anhydrase, and active transport of HCO_3^- (Gao and McKinley, 1994; Raven, 1997; Larsson and Axelsson, 1999; Riebesell et al., 2000). Due to the low diffusion rate of CO_2 in seawater, most macroalgae directly absorb HCO_3^- rather than CO_2 (Hurd et al., 2014). Seaweeds possess carbon-concentrating mechanisms (CCMs), and these CCMs are increasingly important because levels of HCO_3^- have been rising in seawater during the past few decades (Millero et al., 2002; Raven and Beardall, 2014). Studies of CCMs are much more limited in marine macroalgae compared with phytoplankton (Bowes, 2011; Lachmann et al., 2016; Xu et al., 2017).

Giant brown seaweeds predominantly inhabit cold and temperate seawater with dim light and limited dissolved inorganic carbon (DIC) concentrations. Many brown algae form kelp forests in deep waters and may have a net annual primary productivity of up to 3 kg C m^{-2} (Abdullah and Fredriksen, 2004; Hurd et al., 2014). This productivity may be attributed to co-function of the Calvin cycle and C_4 pathways,

---

[*] Corresponding author. CAS Key Laboratory of Experimental Marine Biology, Institute of Oceanology, Chinese Academy of Sciences, No.7 Nanhai Road, Qingdao, 266071, China.

E-mail address: dlduan@qdio.ac.cn (D. Duan).

https://doi.org/10.1016/j.plaphy.2019.01.032
Received 14 September 2018; Received in revised form 28 January 2019; Accepted 30 January 2019

Abbreviations

AAT	Aspartate aminotransferase
ALT	Alanine transaminase
CCM	Carbon-concentrating mechanism
DIC	Dissolved inorganic carbon
ER	Endoplasmic reticulum
FBA	Fructose-1,6-bisphosphate aldolase
FBP	Fructose-1,6-bisphosphatase
FW	Fresh weight
GAPDH	Glyceraldehyde-3-phosphate dehydrogenase
KEGG	Kyoto Encyclopedia of Genes and Genomes
MDH	Malate dehydrogenase
ME	Malic enzyme
NAD-ME	NAD-dependent malic enzyme
NADP-ME	NADP-dependent malic enzyme
OAA	Oxaloacetate
ORF	Open reading frame
PEPC	Phosphoenolpyruvate carboxylase
PEPCK	Phosphoenolpyruvate carboxykinase
PGK	Phosphoglycerate kinase
PK	Pyruvate kinase
PPDK	Pyruvate phosphate dikinase
PRK	Phosphoribulokinase
RPE	Ribulose-phosphate 3-epimerase
RPI	Ribose-5-phosphate isomerase
Rubisco	Ribulose-1,5-bisphosphate carboxylase/oxygenase
SBP	Sedoheptulose-1,7-bisphosphatase
TAL	Transaldolase
TKL	Transketolase
TPI	Triose phosphate isomerase

which has been reported in Fucales and Laminariales (Küppers and Kremer, 1978; Kremer, 1981). For example, ^{14}C isotopic tracing analysis in *Fucus* and *Laminaria* showed that ^{14}C accumulates in C_4 acids (Ji et al., 1980; Bidwell and Mclachlan, 1985). Cabello-Pasini and Alberte (2001) detected the C_4-related enzymatic activities in *Laminaria setchellii* and reported different carboxylation pathways in its thallus. Although genome and transcriptome data are available (Cock et al., 2010; Ye et al., 2015), whether an inducible C_4-like metabolism exists in brown algae remains unclear (Gravot et al., 2010; Bi and Zhou, 2016).

Saccharina japonica is one of the most important cultivated brown seaweed species. Carbohydrates may account for as much as 60% of its dry weight, and we presume that kelp may possess relatively efficient inorganic carbon fixation pathways considering that it fixes DIC to build complex carbon-based molecules. Wang et al. (2011) previously proposed the possible existence of a C_4-like pathway in *S. japonica* by comparing ribulose-1,5-bisphosphate carboxylase/oxygenase (Rubisco) activity in different generations of the organism. An annotation of C_4-related genes from the *S. japonica* transcriptome database indicated the possible existence of a C_4-like pathway (Wang et al., 2013). Chi et al. (2014) analyzed the phylogenetic relationships of C_4-related genes from 19 Phaeophyceae species. However, the above evidence is not sufficient to show that C_4 photosynthesis functions in *S. japonica*. It is required to show evidence for expression of these enzymes in an intracellular location compatible with C_4 photosynthesis and their response to different carbon, light or temperature conditions (Gowik and Westhoff, 2011; Xu et al., 2012; Raven and Giordano, 2017). In this study, we screened genes encoding enzymes in the Calvin cycle and C_4 pathways through a genome-wide survey in *S. japonica* and predicted their subcellular localization. We investigated the responses of putative C_4-related enzymes to bicarbonate concentrations and light intensity. Our results provided explanations for the physiological factors underpinning the rapid growth and strong environmental adaptability of this kelp.

2. Materials and methods

2.1. Algal sample treatment

Juvenile sporophytes of *S. japonica* (ca.50 cm in length and ca. 5 cm in width) were collected from cultivated rafts in April 2017 in Rongcheng, Shandong, China. Robust samples were selected and rinsed with filtered seawater several times and precultured in sterilized seawater enriched with 11.76 μM $NaNO_3$ and 7.35 μM KH_2PO_4 at 15 °C in darkness overnight. To explore the effects of bicarbonate availability, the individual sporophytes were similarly exposed to solutions with different concentrations of bicarbonate (0 and 0.1 M $KHCO_3$ added into sterilized seawater) for 2 h. To explore the influence of light intensity, the individual sporophytes were exposed to different irradiances (0 and 100 $\mu mol\ m^{-2}\ s^{-1}$) for 6 h.

2.2. RNA extraction and cDNA synthesis

Total RNA extraction was performed using an RNeasy Plant Mini Kit following the manufacturer's instructions (Qiagen, Germany). RNA was quantified with a Nanodrop 2000 Spectrophotometer (Thermo Scientific, USA), and RNA quality was verified with 1% agarose gel electrophoresis. First-strand cDNA was synthesized using a PrimeScript II cDNA Synthesis Kit (Takara, Japan) and stored at −20 °C for the subsequent gene cloning and quantitative real-time PCR (qRT-PCR) analysis.

2.3. Sequence analysis of carbon fixation-related genes

We screened C_3 and C_4 pathway-related unigenes from our *S. japonica* genome libraries in the NCBI database (Accession: MEHQ00000000). The amino acid sequences from these genes were then aligned with the NCBI database using the BLASTP algorithm. The online software SMART was used to screen the protein modular architecture (PFAM domains), signal peptides and transmembrane helices (Letunic et al., 2015; Letunic and Bork, 2017). HECTAR v1.3 and TargetP jointly predicted possible localizations to the plastid, mitochondrion and cytoplasm etc. (Emanuelsson et al., 2007; Gschloessl et al., 2008). C-terminal retention signals (KDEL, DDEL or DEEL) were manually identified in endoplasmic reticulum (ER) proteins. Enzymes without recognizable targeting sequences were regarded as cytosolic or targeted to other cellular compartments.

2.4. Determination of cellular contents of chlorophyll *a*

The chlorophyll *a* content was measured for subsequent determination of enzyme activity. ~0.1 g fresh tissue was ground with liquid nitrogen and then transferred to a 2 mL centrifuge tube with 80% (V/V) acetone. The tube was centrifuged at 4000 rpm for 15 min after incubation in darkness for 5 min. The supernatant was then transferred to a volumetric flask, and 80% acetone was added to a total volume of 10 mL. Absorbance was measured at 630, 647 and 664 nm with a microplate spectrophotometer (Eon, BioTek, USA). The concentration of chlorophyll *a* (chl*a*) was calculated using the following formula (Guo et al., 2015):

$$\text{chl}a\ (\text{mg/l}) = 11.85A_{664} - 1.54A_{647} - 0.08A_{630}$$

2.5. Transcriptional profiles of putative C_4-related genes

Using Primer Premier 5 software, we designed the specific primers for the Rubisco large subunit gene, and genes involved in possible C_4 pathways: MDH, ME, PEPC, PEPCK and PPDK. The transcriptional levels of each gene were normalized against those of β-actin (Accession: FJ375360.1). qRT-PCR detection was performed with a SYBR *Premix Ex Taq*™ II kit (Takara, Japan) using a TP800 Thermal Cycler Dice™ (Takara, Japan). A total volume of 25 μL of a mixture containing 12.5 μL of Premix, 1 μL of each primer (10 μM), 2 μL of diluted cDNA and 8.5 μL of RNase-free water was prepared for each reaction. Each sample was amplified using a standard PCR protocol consisting of 95 °C for 10 s, followed by 40 cycles of 95 °C for 5 s, 58 °C for 30 s, and 72 °C for 30 s. Triplicate technical replicates were performed independently, and relative quantitative values were calculated by the $2^{-\triangle\triangle Ct}$ method (Schmittgen et al., 2000).

2.6. Detection of the endogenous activities of putative C_4-related enzymes

Total crude protein was extracted from approximately 0.2 g of kelp sample (fresh weight, FW) in 1 mL of ice-cold Bicine-KOH (1 M, pH 9.0) solution containing 5 mM DTT and protease inhibitors (modified from Osorio et al., 2014). After incubation in an ice bath for 20 min, the homogenate was centrifuged at 12,000 rpm for 5 min. The supernatant was transferred to new tubes for the measurement of PEPCK and PEPC. The carboxylation and decarboxylation activities of PEPCK were measured in HEPES buffer (100 mM, pH 7.0) and Tris-acetate buffer (65 mM, pH 7.4), respectively (Walker et al., 2002). PEPC activity was determined by placing 20 μL of extract in 1 mL of EPPS-NaOH buffer (100 mM, pH 8.0) according to the method described by Cousins et al. (2007), and *Chlorophytum comosum* served as a positive control.

For the MDH, ME, and pyruvate orthophosphate dikinase (PPDK) activity measurements, approximately 0.1 g (FW) of sample was ground and homogenized in prechilled 100 mM Tris-HCl (pH 8.3) extraction solution containing 5 mM DTT, 2 mM EDTA and protease inhibitors. The homogenate was placed in an ice bath for 20 min and then centrifuged at 12,000 rpm for 5 min at 4 °C. MDH activity was determined in Tris-HCl buffer (50 mM, pH 7.8) containing 2 mM $MgCl_2$, 0.5 mM EDTA, 0.2 mM NADH/NADPH and 2 mM OAA. The conversion of malate to pyruvate by ME was assayed in 50 mM Tris-HCl (pH 7.8) buffer with 50 mM l-malate and 1 mM NAD^+/$NADP^+$ (Freschia et al., 2010). PPDK activity was detected using an assay mixture containing 50 mM Tris-HCl (pH 8.3), 6 mM $MgSO_4$, 10 mM DTT, 1 mM PEP, 1 mM trisodium phosphate, 0.15 mM NADH, 1 mM AMP and 2 U/mL lactic dehydrogenase according to the method of Xu et al. (2012).

The total protein was quantified with an Easy Protein Quantitative Kit (TransGen, Beijing, China) according to the Bradford method (Bradford, 1976). A 200 μL mixture containing 100 μL of enzyme extracts was used for each assay. The activity was initiated by adding different substrates and was measured in a continuous assay at 26 °C. The OD_{340} absorption value was detected at 10 min using a PowerWave HT microplate spectrophotometer. A mixture without enzyme extracts was used for each assay as a negative control.

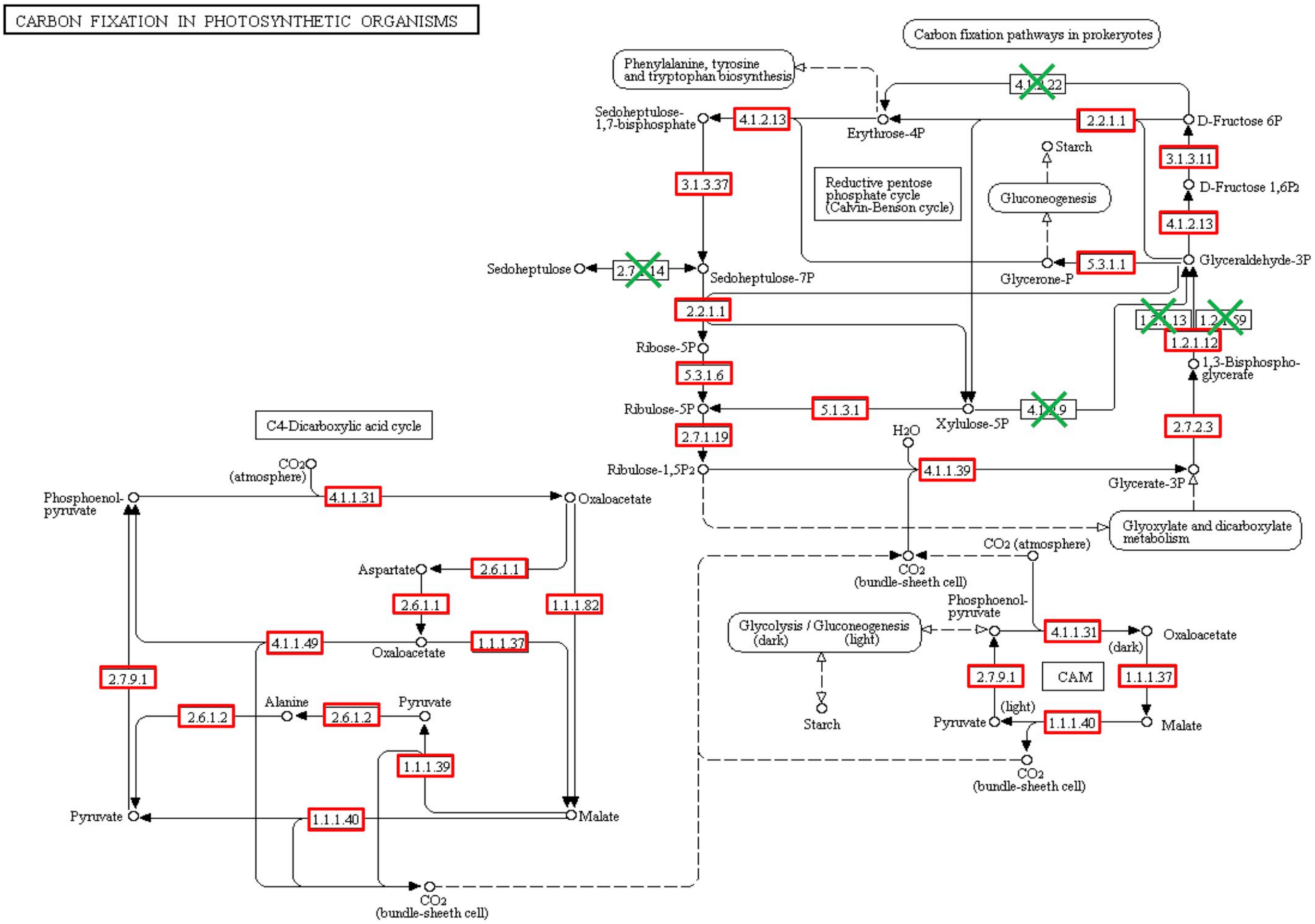

Fig. 1. Carbon fixation pathway in *Saccharina japonica* generated by KEGG (Accession: PRJNA148185). The red rectangle represents genes annotated from the *S. japonica* genome database (Accession: MEHQ00000000). The green cross indicates the absence of the enzyme. The numbers in rectangles are the EC numbers of the enzymes. (For interpretation of the references to colour in this figure legend, the reader is referred to the Web version of this article.)

3. Results

3.1. Annotation and sequence analysis of carbon fixation related genes in S. japonica

In total, 56 genes involved in the carbon fixation pathways were screened. The schematic domain architecture of these enzymes is shown in Fig. S1 and Fig. S2, which indicates the presence of signal peptides, transmembrane helices and conserved motifs. Except for the sedoheptulokinase, fructose-6-phosphate phosphoketolase and phosphoketolase genes, all the other enzymes involved in the Calvin cycle, C_4-Dicarboxylic acid cycle and CAM pathway were found according to the Kyoto Encyclopedia of Genes and Genomes (KEGG) database (Fig. 1). The annotated genes were verified by the BLASTX algorithm, and 40 of these 56 sequences (71%) contained complete open reading frames (ORFs) (Table S1). With 5′ and 3′ RACE-PCR, we cloned the full-length CDS of 10 putative C_4-related genes and submitted the nucleic acid sequences to GenBank (Table 1). Approximately 93% of the genes were highly similar (average 80% identities) to sequences of genes from brown algae, including *Ectocarpus siliculosus*, *Dictyota dichotoma*, *Undaria pinnatifida*, *S. sculpera* and *Scytosiphon lomentaria* (Table S1). The amino acid sequences of all 56 genes are listed in Table S2. The PFAM domains screened by SMART software verified the correct annotations of each sequence (Figs. S1 and S2). Specifically, for C_4-related enzymes, the presumed PEPC sequence (Accession: AIW62922.1) contains two PEPCase domains. The Aminotran_1_2 motifs are observed in 7 AAT sequences, and AAT3, AAT5 and AAT6 contain the DegT_DnrJ_EryC1 domain, which indicates that they belong to a pyridoxal-phosphate-dependent aminotransferase family. The predicted MDH enzymes (Accession: AIW62923.1 and AIW62924.1) have conventional Ldh_1 motifs, and MDH1 contains a transmembrane helix at its N-terminus. The presence of a PEPCK_ATP motif indicates that the predicted PEPCK (Accession: AIW62929.1) is ATP-dependent. NADP-ME and NAD-ME (Accession: AIT70137.1 and AIW62930.1, respectively) contain the same motifs and show the presence of N-terminal (Malic) and NAD-binding domains (Malic_M) of MEs. The predicted PPDK (Accession: AIW62928.1) is comparable to the C_4-type PPDK protein in *Zea mays* (Accession: ADC32810.1) but lacks one N-terminal targeting sequence.

Fig. 2 shows the sequence alignments of crucial C_4 pathway-related enzymes (PPDK, PEPC, PEPCK and ME) in typical stramenopile species: *S. japonica*, *E. siliculosus* and *Thalassiosira pseudonana*. An alignment of the PPDK sequences shows that the expected catalytic histidine residue is present in the conserved region of GGMTSHAAVVAR. The residues at the PEP-binding site (R … R … D … R … E … ND … R … C) are conserved in stramenopile species (Fig. 2a). The predicted PEPC contains glutamate 491 and arginine 496, which are two tetramer-related amino acids (Fig. 2b). A conserved serine residue is found in *S. japonica* and *E. siliculosus* at positions homologous to S780 in *Z. mays* (Accession: ACJ38542.1), and this represents a typical characteristic for C_4-specific PEPC genes (Fig. 2b). The predicted PEPCK sequence contains a series of active sites, e.g., OAA-binding sites (R…Y⋯K…R), ATP-binding sites (H⋯K…R) and Mg^{2+}-binding sites (R … I … T) (Fig. 2c). *S. japonica* possesses two ME sequences that both have five highly conserved regions (I ~ V) (Fig. 2d). Three adjacent residues (GNN) in NADP-ME are responsible for binding NAD(P) in *S. japonica* and *E. siliculosus*, relative to SNN in NAD-ME from *S. japonica* and the CNN in malic enzyme in *T. pseudonana* (Fig. 2d).

3.2. Subcellular targeting prediction of C_4-related enzymes

The predicted intracellular targeting of *S. japonica* carbon fixation enzymes is summarized in Table S3. Except for phosphoribulokinase (PRK), we find that other Calvin cycle enzymes contain at least one entry to be localized in the chloroplast using HECTAR prediction. The presence of phenylalanine at cleavage sites provides further evidence for the localization of these enzymes in the plastid (Table S3). On the other hand, the putative C_4-related enzymes PEPC, AAT6, MDH2, PEPCK, NAD-ME and ALT are predicted to localize to the mitochondrion. Similar to the Calvin cycle enzymes, the chloroplast-localized pyruvate kinase (PK1) and PPDK also contain phenylalanine at the cleavage sites. Based on these predictions of subcellular localization, we deduced the compartmentation of the carbon fixation pathways in *S. japonica* (Fig. 3). In the chloroplast, pyruvate is catalyzed by PPDK to yield PEP. Three entries annotated as PEP/phosphate translocator were listed in Table S1, which all contain 7-10 transmembrane helices for their location in membranes. Therefore, plastid PEP is transported to the mitochondrion through PEP translocators and then carboxylated via PEPC to form OAA. OAA is either decarboxylated by PEPCK or catalyzed by MDH2 and NAD-ME to release CO_2 (Fig. 3). We presumed that the enriched CO_2 could diffuse to the plastid and initiate the Calvin cycle from the production of glycerate-3-phophate (3-PG) to the regeneration of RuBP (Fig. 3).

Furthermore, we compared the types, numbers and localizations of the annotated C_4-related genes in *S. japonica* with those of their orthologues in *E. siliculosus*, *Phaeodactylum tricornutum* and *T. pseudonana* (Table 2). The putative C_4-related genes are present in greater abundance in *E. siliculosus* and *S. japonica* than in diatoms, especially for ME and MDH isozymes. ME and PEPCK were identified as mitochondrion-targeted proteins in the four stramenopiles species, indicating that they may produce CO_2 in mitochondria through a C_4-like pathway. PEPC and MDH are also predicted to be located in mitochondria, suggesting that the production of OAA and malate and their subsequent decarboxylation both occur in mitochondria. In addition, ALT is predicted to catalyze the interconversion of pyruvate and alanine in mitochondria, thereby regulating the ME activity and indirectly compensating the pyruvate in the chloroplast.

Table 1

The sequence features of putative C_4-and CAM-related genes from *Saccharina japonica*.

EC number	Enzyme name	Abbreviation	CDS (bp)[a]	genome ID	Blastp accession[b]/identities[b]	Length (aa)	Accession[c]
EC 4.1.1.31	phosphoenolpyruvate carboxylase	PEPC	2856/2850	MRNA_029840	AIT70056.1/84%	949	AIW62922.1
EC 2.6.1.1	aspartate aminotransferase 1	AAT1	999/1371	MRNA_001797	AIT70206.1/72%	456	AIW62925.1
		AAT2	1206/1206	MRNA_018179	AIT70232.1/99%	401	AIW62926.1
EC 1.1.1.37	malate dehydrogenase	MDH1	1293/1218	MRNA_003134	AIT70174.1/84%	405	AIW62923.1
		MDH2	1050/1050	MRNA_002455	AIT70171.1/97%	349	AIW62924.1
EC 4.1.1.49	phosphoenolpyruvate carboxykinase	PEPCK	681/1734	MRNA_015129	CBJ26625.1/90%	577	AIW62929.1
EC 1.1.1.39	NAD-malic enzyme	NAD-ME	1749/2103	MRNA_023832	AIT70134.1/98%	700	AIW62930.1
EC 1.1.1.40	NADP-malic enzyme	NADP-ME	1686/1686	MRNA_001190	AIT70133.1/99%	561	AIT70137.1
EC 2.6.1.2	alanine transaminase	ALT	1506/1506	MRNA_018184	AIT69925.1/99%	501	AIW62927.1
EC 2.7.9.1	pyruvate orthophosphate dikinase	PPDK	2970/2970	MRNA_019490	AIT69955.1/89%	989	AIW62928.1

[a] The left number is the length of CDS from genome sequencing; the right number is the length of ORF from gene cloning in this study.

[b] The left ID is the NCBI accession number of entries showing the highest identities with our sequences; the right number is the percentage of identities.

[c] The accession number of our putative C_4-related genes.

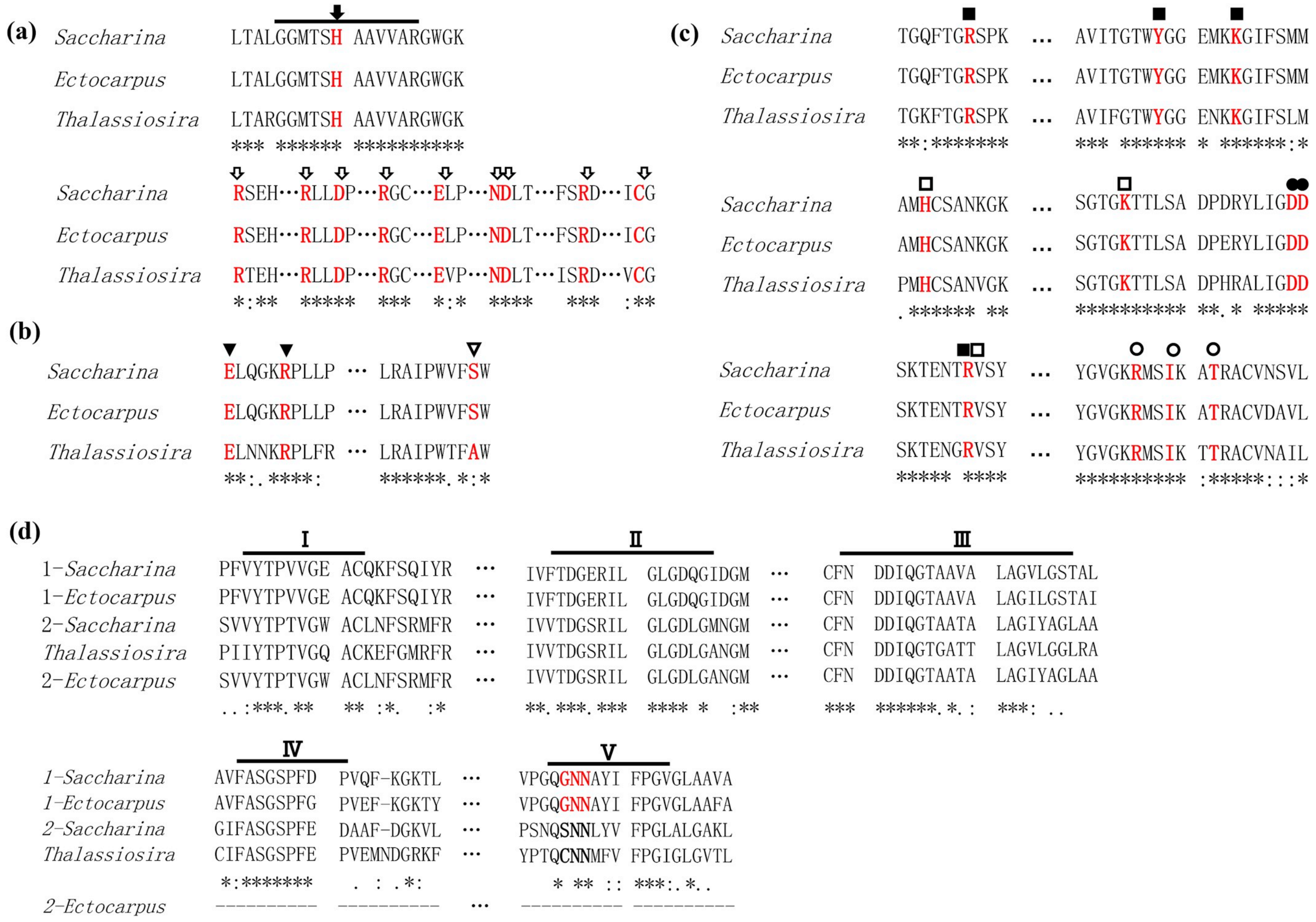

Fig. 2. Sequence alignments of C_4 enzymes (PPDK, PEPC, PEPCK and ME) in typical stramenopile species. **a** PPDK sequence alignment shows the conserved region containing the histidine (H) residue (solid arrow) responsible for catalysis and the residues at the PEP-binding site (hollow arrows). **b** PEPC sequences contain the tetramer-related amino acids glutamate (E) and arginine (R) (solid triangles) and the serine (S) residue (hollow triangle) that is a typical characteristic for C_4-specific PEPC genes. **c** PEPCK sequences contain conserved active sites: solid squares show OAA-binding sites; hollow squares indicate ATP-binding sites; solid circles indicate adenine-binding sites; hollow circles show Mg^{2+}-binding sites. **d** Five conserved regions in both NAD-ME and NADP-ME and the three adjacent residues (GNN) in NAD-ME responsible for binding NAD in these enzymes in *S. japonica* and *E. siliculosus*. The number before the species name refers to an enzyme: 1, NADP-ME; 2, NAD-ME.

3.3. Transcriptional profiles of C_4-related genes in response to HCO_3^- concentration and light intensity

Seven pairs of primers for putative C_4-related genes and one pair of primers for the large subunit of Rubisco (rbcL) were designed (Table S4) to detect transcriptional variations under various HCO_3^- concentrations and light intensities. Fig. 4 shows the different expression levels of putative C_4 genes. The levels of *PPDK* transcript were increased by 13.9-fold at a low HCO_3^- concentration (without addition of $KHCO_3$). *NADP-ME*, *MDH1* and *PEPCK* transcription was 2.3-, 1.5- and 1.3-fold greater at 0 M $KHCO_3$ than at 0.1 M $KHCO_3$, respectively (Fig. 4a). On the contrary, the transcriptional levels of *NAD-ME* and *PEPC* were 2.3- and 4.5-fold lower at 0 M $KHCO_3$ than at 1 M $KHCO_3$, respectively (Fig. 4a). Similarly, the abundance of *rbcL* was hundreds of times higher than that of all C_4-related genes, and its expression levels were increased by 3.9-fold after HCO_3^- enrichment (Fig. S3a). Juvenile sporophytes were incubated under darkness and light (100 μmol m^{-2} s^{-1}) for 6 h and the mRNA levels of *MDH1*, *MDH2*, *NAD-ME* and *PEPCK* were relatively greater in darkness than under light, and presented values that were 33.1-, 2.2-, 3.6- and 1.5-fold higher, respectively (Fig. 4b). In contrast, *PPDK* was highly transcribed when the sporophytes were subjected to light and exhibited 12.7-fold more transcripts under light than in darkness (Fig. 4b). The expression levels of *rbcL* were similarly increased by 2.1-fold after exposure to light (Fig. S3b).

3.4. Enzymatic activities in response to HCO_3^- concentrations and light intensities

Fig. S4 shows that the chlorophyll *a* content is increased either by adding $KHCO_3$ to the culture or raising the light intensity. The initial activities of each C_4-related enzyme in response to light and $KHCO_3$ treatment were calculated by measuring the variation in OD_{340} relative to the kelp fresh weight, the Chl*a* weight and total protein content (Figs. 5 and S5). NAD-ME and PEPCK decarboxylation activities were the highest among all the C_4-related enzymes under these bicarbonate and light treatments (Fig. 5). The addition of $KHCO_3$ barely changed the activities of MDH, ME and PEPCK but dramatically decreased the PPDK activity by 36.5-fold (Fig. 5a). Similarly, PPDK activity was most affected by light and presented 4.8-fold higher values under light irradiance than in darkness (Fig. 5b). NAD-ME activity was 1.3-fold higher under light, while PEPCK decarboxylation activity was 1.3-fold higher in darkness. NADH-MDH and NADP-ME activities were relatively low under both treatments. The carboxylation activities of PEPC, NADPH-MDH and PEPCK were detected but only at negligible levels (data not shown).

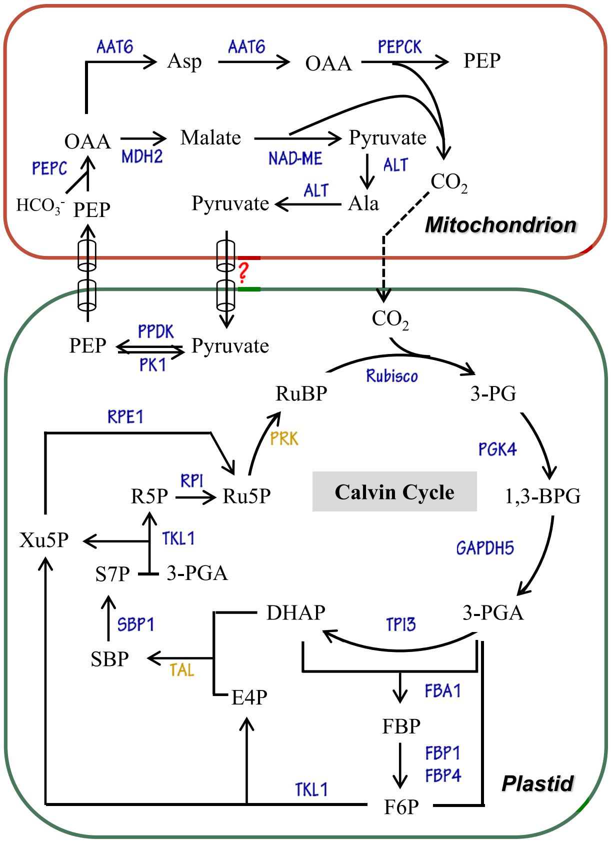

Fig. 3. Proposed model of carbon fixation metabolism in *Saccharina japonica* based on annotations and the subcellular location of carbon fixation proteins. Enzyme abbreviations: AAT, aspartate aminotransferase; ALT, alanine transaminase; FBA: fructose-1,6-bisphosphate aldolase; FBP: fructose-1,6-bisphosphatase; GAPDH: glyceraldehyde-3-phosphate dehydrogenase; MDH, malate dehydrogenase; ME, malic enzyme; PEPC, phosphoenolpyruvate carboxylase; PEPCK, phosphoenolpyruvate carboxykinase; PGK: phosphoglycerate kinase; PK, pyruvate kinase; PPDK, pyruvate phosphate dikinase; PRK: phosphoribulokinase; RPE: ribulose-phosphate 3-epimerase; RPI: ribose-5-phosphate isomerase; Rubisco, ribulose-1,5-bisphosphate carboxylase/oxygenase SBP: sedoheptulose-1,7-bisphosphatase; TAL: transaldolase; TKL: transketolase; TPI: triose phosphate isomerase.

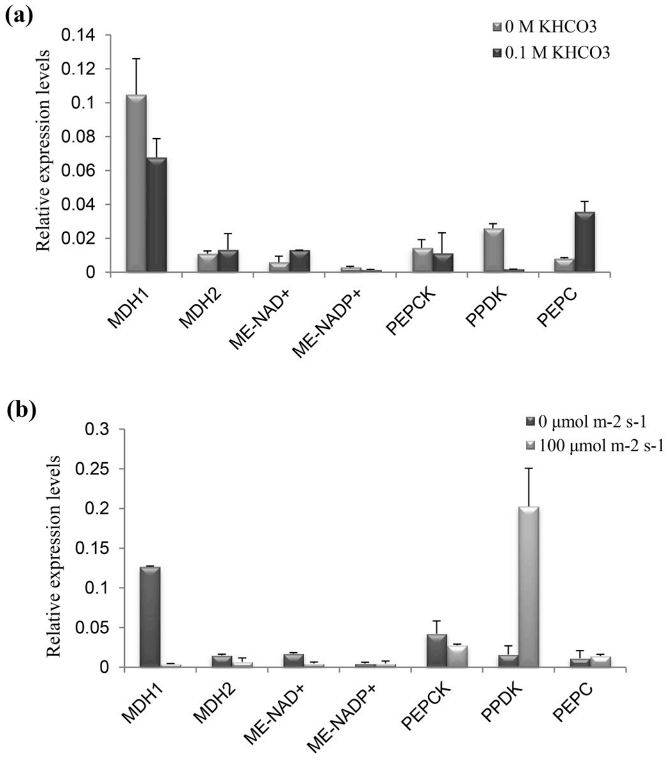

Fig. 4. Transcriptional profiles of putative C$_4$-related genes isolated from individual *Saccharina japonica* kelps at various KHCO$_3$ concentrations (**a**) and light intensities (**b**).

Comparative profiles of transcription and enzymatic activities of each C$_4$-related gene are summarized in Fig. 6. The relative transcriptional levels of most enzymes (PPDK, PEPCK and MDH) are consistent with their related activities. PPDK is the only protein whose mRNA and activity levels are up-regulated by light and the lower HCO$_3^-$ concentration. PEPCK and MDH are up-regulated in darkness and at the lower HCO$_3^-$ concentration. The NAD-ME decarboxylation activity decreased at the lower HCO$_3^-$ concentration but increased with light intensity.

Table 2
Comparison of the amounts, lengths, and localizations of C$_4$-related genes from *Phaeodactylum tricornutum*, *Thalassiosira pseudonana*, *Ectocarpus siliculosus* and *Saccharina japonica*.

	P. tricornutum		*T. pseudonana*			*E. siliculosus*		*S. japonica*	
Abbreviation	ID[a]	Localization	Protein ID[b]	Localization[d]	Localization[e]	Protein ID[c]	Localization	Protein ID[c]	Localization
PEPC	56026 20853	ER/PPS? Mitochondria	B8C1R7 B8BYW8	CER/PPS Mitochondria	Cytosol Mitochondria	CBN73928.1	Mitochondria	AIW62922.1	Mitochondria
ME	56501	Mitochondria	B8C1Z0	Mitochondria	Cytosol	CBJ25596.1	No target peptide	AIT70137.1	No target peptide
						CBN77654.1 CBN77656.1	Mitochondria No target peptide	AIW62930.1	Mitochondria
PEPCK	23074	Mitochondria	B8C274	Mitochondria	Mitochondria	CBJ26625.1	Mitochondria	AIW62929.1	Mitochondria
MDH	51297	Mitochondria	B5YNR1	Mito or CER	–	CBJ30671.1	Signal peptide	AIW62923.1	No target peptide
			B8BQC2	CER or Mito		CBN78787.1 CBJ32518.1	Mitochondria No target peptide	AIW62924.1	Mitochondria
PPDK	21988	Plastid	B8C332	Cytosol	Cytosol	CBN74442.1	No target peptide	AIW62928.1	Plastid
ALT	–	–	B8C017	Cytosol	–	CBJ31990.1	Mitochondria	AIW62927.1	Mitochondria

References: *P. tricornutum*: Kroth et al. (2008); *T. pseudonana*: Kustka et al. (2014); Tanaka et al. (2014); *E. siliculosus*: Gravot et al. (2010).

[a] Protein IDs for *P. tricornutum* were from the Phatr2 JGI database.

[b] Protein IDs for *T. pseudonana* were from the UniProt database.

[c] Protein IDs for *E. siliculosus* and *S. japonica* were from the NCBI database.

[d] Potential localization of C$_4$ enzymes from the results of Kustka et al. (2014).

[e] Potential localization of C$_4$ enzymes from the results of Tanaka et al. (2014).

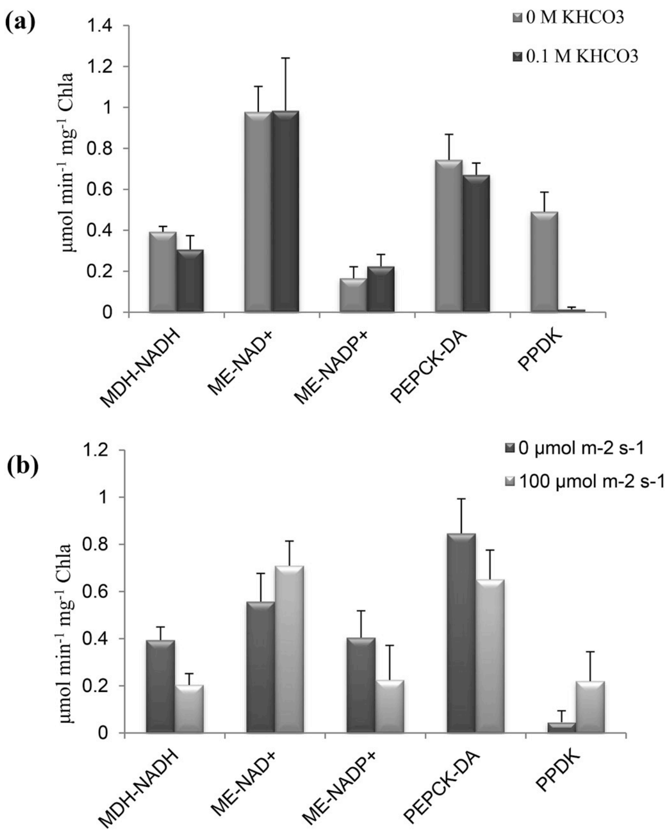

Fig. 5. Initial activity of different enzymes under various $KHCO_3$ concentrations and light irradiance. Enzymatic activities were calculated relative to kelp fresh weight, chlorophyll *a* weight and total protein content. **a** C_4-related enzymatic activity at different concentrations of $KHCO_3$. **b** C_4-related enzymatic activity at different light intensities. Error bars represent the SD of three replicates.

4. Discussion

4.1. Correlation between protein sequences and their putative functions

Highly conserved amino acids were identified in the predicted PPDK, PEPC, ME and PEPCK sequences in *S. japonica* (Fig. 2). We found a series of residues responsible for binding PEP in all the selected stramenopile PPDK sequences that matched those residues in the C_4-PPDK from *Flaveria trinervia* (Minges et al., 2017). This result indicated the potential activity of PPDK for PEP regeneration in stramenopile species. The two key residues (Glu491 and Arg496) responsible for tetramerization in *S. japonica* PEPC were believed to reduce its affinity for its substrate (PEP), which may explain the negligible PEPC activity detected in the kelp. Similar behavior has been reported in maize and diatoms (Wedding et al., 1994; Trimborn et al., 2009). We confirmed the presence of conserved substrate-binding, magnesium-chelating and coenzyme-binding residues in the *S. japonica* PEPCK sequence, and their presence strongly suggests that this mitochondrial PEPCK is an active enzyme catalyzing the decarboxylation reaction. Conserved region I exists in putative NAD-ME and NADP-ME sequences. Long et al. (1994) reported that region I utilizes both NAD^+ and $NADP^+$ and that $NADP^+$ is used less efficiently. However, glycine was replaced with a serine in NAD-ME (Fig. 2d). Considering that NAD is bound by the oxygen of the carboxyl group, we presumed that this substitution would not affect its activity. The two *S. japonica* MEs are therefore likely to have decarboxylating activity and prefer NAD^+ over $NADP^+$. The enzymatic activity analysis showed that ME activity in the kelp was much higher with NAD^+ than with $NADP^+$ (Fig. 5), which might be explained by the preference of NAD-binding site.

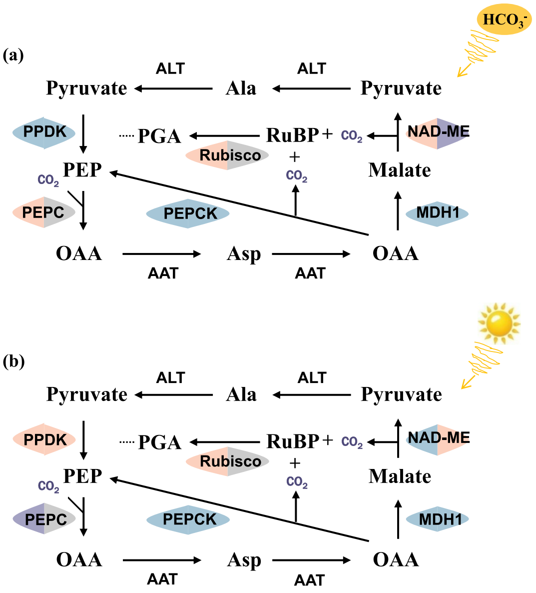

Fig. 6. Comparative analysis of transcriptional profiles and enzymatic activity in *S. japonica*. The block on the left indicates the gene expression levels of each presumed enzyme, and the block on the right shows the corresponding activity. **a** Comparison of samples exposed to 0 M and 0.1 M $KHCO_3$, respectively. **b** Comparison of samples exposed in the darkness and 100 μmol m^{-2} s^{-1} light intensity. Pink indicates 'up-regulation' and blue means 'down-regulation'. Gray indicates activities that were not measured and cases where only trace amounts of activity were observed. Purple indicates that no obvious changes were detected. (For interpretation of the references to colour in this figure legend, the reader is referred to the Web version of this article.)

4.2. Subcellular localization of carbon fixation pathways

Unlike the C_4 cycle, which depends on dimorphic chloroplasts and was identified in Suaedoideae (Edwards and Voznesenskaya, 2011), the C_4-related enzymes in *S. japonica* may utilize the compartmentation of plastids and mitochondria to concentrate CO_2 (Table 2; Fig. 3). The chloroplast-targeting of PPDK is consistent with diatom PPDKs catalyzing the production of PEP (Kroth et al., 2008). In this study, transporters for PPDK substrate—pyruvate were not successfully annotated from *Saccharina* genome, which is also the same case for diatoms (Fig. 1 in Kroth et al., 2008). Bi and Zhou (2016) produced a schematic diagram for carbonic anhydrases and C_4 pathways and tentatively proposed that PEPCK and PEPC were localized in the cytosol. We annotated mitochondrion-localized PEPCK and PEPC in the *S. japonica* genome. The mitochondrion localization of PEPCK is consistent with its localization in diatoms but not most eukaryotes, which have both mitochondrial and cytosolic PEPCK isoforms (Yang et al., 2009; Tanaka et al., 2014). The lack of a cytosolic PEPCK indicates that CO_2 might not be produced in the cytoplasm. The single mitochondrial PEPC is different from the case in diatoms, which possess another ER/PPS-localized PEPC (Kustka et al., 2014; Tanaka et al., 2014). The mitochondrial MDH and NAD-ME complete the pathway from OAA to pyruvate. With regard to all these *S. japonica* enzymes localizing in mitochondria, we presume that the secondary endosymbiotic mitochondria have been undervalued in previous photosynthetic studies in stramenopiles.

4.3. Influence of HCO_3^- and light intensity on putative C_4-related enzymes

PEPCK and NAD-ME decarboxylation activity was the highest of all the C_4-related enzymes. PEPCK is up-regulated at low HCO_3^- concentrations to supply carbon for Rubisco, but its transcription was less sensitive to light intensity. NAD-ME had a much higher activity than NADP-ME, but its insensitivity to HCO_3^- and light variations indicated that MEs are not as essential for CO_2 production as PEPCK. Although

PPDK was not the most active among these enzymes, it presented the greatest response to low bicarbonate levels and high light intensity through increasing transcription and enzymatic activity. The model diatom species *P. tricornutum* and *T. pseudonana* were reported to possess a set of C_4-related enzymes (Kroth et al., 2008), but their PPDKs have little effect on photosynthesis (Haimovich-Dayan et al., 2013; Kustka et al., 2014). In contrast, PDDK in *S. japonica* responded to low HCO_3^- concentrations. The up-regulation of PPDK indicated that more PEP might be generated for greater assimilation of HCO_3^- in this giant kelp. The co-increase in MDH and PEPCK decarboxylation activity under low HCO_3^- conditions could release more CO_2 and guarantee a relatively high ability of carbon assimilation and fixation.

Kelp habitats typically experience low light intensity (less than 1500 lx, approximately 30 μmol m^{-2} s^{-1}) (Huang and Yi, 1998). In our study, the transcriptional level and activity of PPDK were approximately 13- and 5-fold higher under illumination (100 μmol m^{-2}) than in darkness, respectively. The increase in PPDK activity is comparable to the up-regulation of Rubisco carboxylase activity under light irradiance in our previous report (Shao et al., 2014). With regard to the co-increase of Rubisco and PEPCK activity, we presume that except for Rubisco, *S. japonica* relies on a PPDK-dependent pathway to maintain the dark reaction process and consequent metabolic pathways in the kelp under high light conditions.

Compared with the differentiation of MCs and BSCs in C_4 higher plants, the lower brown alga *S. japonica* has a relatively simple structure, including cuticle, meristems, cortex and sieve cells, etc. (Fig. S6). Our integrated data describing the subcellular localization of putative C_4-related enzymes and their response to HCO_3^- concentrations and light intensity provided clues that a C_4 pathway may exist in the kelp in which CO_2 is enriched in the mitochondria and then diffuses into the chloroplast for the Calvin cycle. Compared with the PPDK-independent mechanism in diatoms, PPDK in *S. japonica* responded intensely to low HCO_3^- concentrations and high light intensities. The subsequent up-regulation of PEPCK and Rubisco might enable greater CO_2 fixation, thereby allowing the kelp to grow more rapidly than if it merely relied on a C_3 pathway.

Acknowledgements

This work was supported by the Shandong Key Research and Development Program (2018GHY115023), Qingdao National Laboratory for Marine Science and Technology Project (No.2018ASKJ03), Open Foundation of the State Key Laboratory of Bioactive Seaweed Substances, and CAS-Fujian STS Project (2017T3012). The authors are grateful to the suggestions and manuscript revision by Richard Dorrell from the Institut de Biologie de l'Ecole Normale Supérieure.

Appendix A. Supplementary data

Supplementary data to this article can be found online at https://doi.org/10.1016/j.plaphy.2019.01.032.

5. Compliance with ethical standards

Conflict of interest

The authors hereby declare no conflicts of interest.

Author contributions

ZS and DD conceived and designed research. ZS and PZ conducted experiments. WW and JY contributed the cultivation and the collection of kelp samples. WW and FW were involved in data analysis. ZS interpreted the data and wrote the manuscript. DD gave critical revision of the manuscript. All authors read and approved the manuscript.

References

Abdullah, M.I., Fredriksen, S., 2004. Production, respiration and exudation of dissolved organic matter by the kelp *Laminaria hyperborea* along the west coast of Norway. J. Mar. Biol. Assoc. U. K. 84 (5), 887–894.

Bidwell, R.G.S., Mclachlan, J., 1985. Carbon nutrition of seaweeds: photosynthesis, photorespiration and respiration. J. Exp. Mar. Biol. Ecol. 86 (1), 15–46.

Bi, Y.H., Zhou, Z.G., 2016. Absorption and transport of inorganic carbon in kelps with emphasis on *Saccharina japonica*. In: Najafpour, M.M. (Ed.), Applied Photosynthesis-New Progress. InTech Open Publishers, Rijeka, pp. 111–131.

Bowes, G., 2011. Single-cell C_4 photosynthesis in aquatic plants. In: Raghavendra, A.S., Sage, R.F. (Eds.), C_4 Photosynthesis and Related CO_2 Concentrating Mechanisms. Springer, Dordrecht, pp. 63–80.

Bradford, M.M., 1976. A rapid and sensitive method for quantitation of microgram quantities of protein utilizing principle of protein-dye binding. Anal. Biochem. 72, 248–254.

Cabello-Pasini, Alberte, R.S., 2001. Enzymatic regulation of photosynthetic and light-independent carbon fixation in *Laminaria setchellii* (Phaeophyta), *Ulva lactuca* (Chlorophyta) and *Iridaea cordata* (Rhodophyta). Rev. Chil. Hist. Nat. 74 (2), 229–236.

Chi, S., Wu, S.X., Yu, J., Wang, X.M., Tang, X.X., Liu, T., 2014. Phylogeny of C_4-photosynthesis enzymes based on algal transcriptomic and genomic data supports an archaeal/proteobacterial origin and multiple duplication for most C_4-related genes. PLoS One 9 (10) e110154.

CDock, J.M., Sterck, L., Rouzé, P., et al., 2010. The *Ectocarpus* genome and the independent evolution of multicellularity in brown algae. Nature 465, 617–621.

Cousins, A.B., Baroli, I., Badger, M.R., Ivakov, A., Lea, P.J., Leegood, R.C., von Caemmerer, S., 2007. The role of phosphoenolpyruvate carboxylase during C_4 photosynthetic isotope exchange and stomatal conductance. Plant Physiol. 145 (3), 1006–1017.

Doney, S.C., Tilbrook, B., Roy, S., Metzl, N., Le Quéré, C., 2009. Surface ocean CO_2 variability and vulnerability. Deep-Sea Res Pt II 56 (8), 504–511.

Duarte, C.M., Middelburg, J.J., Caraco, N., 2005. Major role of marine vegetation on the oceanic carbon cycle. Biogeosciences 2 (1), 1–8.

Edwards, G.E., Voznesenskaya, E.V., 2011. C_4 photosynthesis: kranz forms and single-cell C_4 in terrestrial plants. In: Raghavendra, A.S., Sage, R.F. (Eds.), C_4 Photosynthesis and Related CO_2 Concentrating Mechanisms. Springer, Dordrecht, pp. 29–61.

Emanuelsson, O., Brunak, S., von Heijne, G., Nielsen, H., 2007. Locating proteins in the cell using TargetP, SignalP and related tools. Nat. Protoc. 2 (4), 953–971.

Freschia, L., Rodriguesa, M.A., Tinéb, M.A.S., Merciera, H., 2010. Correlation between citric acid and nitrate metabolisms during CAM cycle in the atmospheric bromeliad *Tillandsia pohliana*. J. Plant Physiol. 167 (18), 1577–1583.

Gao, K.S., McKinley, K., 1994. Use of macroalgae for marine biomass production and CO_2 remediation: a review. J. Appl. Phycol. 6 (1), 45–60.

Gowik, U., Westhoff, P., 2011. The path from C_3 to C_4 photosynthesis. Plant Physiol. 155, 56–63.

Gravot, A., Dittami, S.M., Rousvoal, S., Lugan, R., Eggert, A., Collén, J., Boyen, C., Bouchereau, A., Tonon, T., 2010. Diurnal oscillations of metabolite bundances and genome analysis provide new insights into central metabolic processes of the brown alga *Ectocarpus siliculosus*. New Phytol. 188 (1), 98–110.

Gschloessl, B., Guermeur, Y., CDock, J.M., 2008. HECTAR: a method to predict subcellular targeting in heterokonts. BMC Bioinf. 9, 393.

Guo, H., Yao, J.T., Sun, Z.M., Duan, D.L., 2015. Effect of temperature, irradiance on the growth of the green alga *Caulerpa lentillifera* (Bryopsidophyceae, Chlorophyta). J. Appl. Phycol. 27 (2), 879–885.

Haimovich-Dayan, M., Garfinkel, N., Ewe, D., Marcus, Y., Gruber, A., Wagner, H., Kroth, P.G., Kaplan, A., 2013. The role of C_4 metabolism in the marine diatom *Phaeodactylum tricornutum*. New Phytol. 197 (1), 177–185.

Huang, H.Z., Yi, J.G., 1998. Study on relation between illumination wavelength and germination, growth of *Laminaria japonica* Aresch gametophyte. Fisheries Sci Technol Inform 25 (6), 265–269 (in Chinese with English abstract).

Hurd, C.L., Harrison, P.J., Bischof, K., Lobban, C.S., 2014. Seaweed Ecology and Physiology, second ed. Cambridge University Press, Cambridge.

Ji, M.H., Pu, S.Z., Ji, X.L., 1980. Studies on the initial products of ^{14}C metabolism in *Laminaria japonica*. Oceanol. Limnol. Sinica 11, 229–240 (in Chinese with English abstract).

Kremer, B.P., 1981. Metabolic implications of non-photosynthetic carbon fixation in brown macroalgae. Phycologia 20 (3), 242–250.

Kroth, P.G., Chiovitti, A., Gruber, A., et al., 2008. A model for carbohydrate metabolism in the diatom *Phaeodactylum tricornutum* deduced from comparative whole genome analysis. PLoS One 3 (1) e1426.

Küppers, U., Kremer, B.P., 1978. Longitudinal profiles of carbon dioxide fixation capacities in marine macroalgae. Plant Physiol. 62 (1), 49–53.

Kustka, A.B., Milligan, A.J., Zheng, H., New, A.M., Gates, C., Bidle, K.D., Reinfelder, J.R., 2014. Low CO_2 results in a rearrangement of carbon metabolism to support C_4 photosynthetic carbon assimilation in *Thalassiosira pseudonana*. New Phytol. 204 (3), 507–520.

Lachmann, S.C., Maberly, S.C., Spijkerman, E., 2016. Ecophysiology matters: linking inorganic carbon acquisition to ecological preference in four species of microalgae (Chlorophyceae). J. Phycol. 52, 1051–1063.

Larsson, C., Axelsson, L., 1999. Bicarbonate uptake and utilization in marine macroalgae. Eur. J. Phycol. 34, 79–86.

Letunic, I., Doerks, T., Bork, P., 2015. SMART: recent updates, new developments and status in 2015. Nucleic Acids Res. 43, 257–260.

Letunic, I., Bork, P., 2017. 20 years of the SMART protein domain annotation resource.

Nucleic Acids Res. 46 (D1), 493–496.

Long, J.J., Wang, J.L., Berry, J.O., 1994. Cloning and analysis of the C_4 photosynthetic NAD-dependent malic enzyme of Amaranth mitochondria. J. Biol. Chem. 269 (4), 2827–2833.

Millero, F.J., Pierrot, D., Lee, K., Wanninkhof, R., Feely, R.A., Sabine, C.L., Key, R.M., Takahashi, T., 2002. Dissociation constants for carbonic acid determined from field measurements. Deep-Sea Res Pt I 49 (10), 1705–1723.

Minges, A., Ciupka, D., Winkler, C., Höppner, A., Gohlke, H., Groth, G., 2017. Structural intermediates and directionality of the swiveling motion of Pyruvate Phosphate Dikinase. Sci Rep-UK 7, 45389.

Nellemann, C., Corcoran, E., Duarte, C.M., Valdés, L., Yong, C., Fonseca, L., Grimsditch, G., 2009. Blue Carbon: A Rapid Response Assessment. United Nations Environment Programme. http://www.grida.no.

Osorio, S., Vallarino, J.G., Szecowka, M., Ufaz, S., Tzin, V., Angelovici, R., Galili, G., Fernie, R., 2014. Extraction and measurement the activities of cytosolic phosphoenolpyruvate carboxykinase (PEPCK) and plastidic NADP-dependent malic enzyme (ME) on tomato (*Solanum lycopersicum*). Bio-protocol 4 (9), 1–7.

Raven, J.A., 1997. Inorganic carbon acquisition by marine autotrophs. Adv. Bot. Res. 27, 85–209.

Raven, J.A., Beardall, J., 2014. CO_2 concentrating mechanisms and environmental change. Aquat. Bot. 118, 24–37.

Raven, J.A., Giordano, M., 2017. Acquisition and metabolism of carbon in the Ochrophyta other than diatoms. Phil Trans R Soc B 372, 20160400.

Riebesell, U., Zondervan, I., Rost, B., Tortell, P.D., Zeebe, R.E., Morel, F.M.M., 2000. Reduced calcification of marine plankton in response to increased atmospheric CO_2. Nature 407 (6802), 364–367.

Schmittgen, T.D., Zakrajsek, B.A., Mills, A.G., Gorn, V., Singer, M.J., Reed, M.W., 2000. Quantitative reverse transcription-polymerase chain reaction to study mRNA decay: comparison of endpoint and real-time methods. Anal. Biochem. 285 (2), 194–204.

Shao, Z.R., Zhang, P.Y., Li, Q.Y., Wang, X.L., Duan, D.L., 2014. Characterization of mannitol-2-dehydrogenase in *Saccharina japonica*: evidence for a new polyol-specific long-chain dehydrogenases/reductase. PLoS One 9 (5), e97935.

Skirrow, G., 1975. The dissolved gases carbon dioxide. In: Riley, J.P., Skirrow, G. (Eds.), Chemical Oceanography. Academic Press, London, pp. 1–92.

Tanaka, R., Kikutani, S., Mahardika, A., Matsuda, Y., 2014. Localization of enzymes relating to C_4 organic acid metabolisms in the marine diatom, *Thalassiosira pseudonana*. Photosynth. Res. 121 (2–3), 251–263.

Trimborn, S., Wolf-Gladrow, D., Richter, K.U., Rost, B., 2009. The effect of $p\mathrm{CO_2}$ on carbon acquisition and intracellular assimilation in four marine diatoms. J. Exp. Mar. Biol. Ecol. 376, 26–36.

Walker, R.P., Chen, Z.H., Acheson, R.M., Leegood, R.C., 2002. Effects of phosphorylation on phospho*enol*pyruvate carboxykinase from the C_4 plant Guinea grass. Plant Physiol. 128 (1), 165–172.

Wang, C., Fan, X.L., Wang, G.C., Niu, J.F., Zhou, B.C., 2011. Differential expression of Rubisco in sporophytes and gametophytes of some marine macroalgae. PLoS One 6 (1), e16351.

Wang, W.J., Wang, F.J., Sun, X.T., Liu, F.L., Liang, Z.R., 2013. Comparison of transcriptome under red and blue light culture of *Saccharina japonica* (Phaeophyceae). Planta 237 (4), 1123–1133.

Wedding, R.T., O'Brien, C.E., Kline, K., 1994. Oligomerization and the affinity of maize phosphoenolpyruvate carboxylase for its substrate. Plant Physiol. 104 (2), 613–616.

Xu, J.F., Fan, X., Zhang, X.W., Xu, D., Mou, S.L., Cao, S.N., Zheng, Z., Miao, J.L., Ye, N.H., 2012. Evidence of coexistence of C_3 and C_4 photosynthetic pathways in a green-tide-forming alga, *Ulva prolifera*. PLoS One 7 (5), e37438.

Xu, K., Chen, H.Z., Wang, W.L., Xu, Y., Ji, D.H., Chen, C.S., Xie, C.T., 2017. Responses of photosynthesis and CO_2 concentrating mechanisms of marin crop *Pyropia haitanensis* thalli to large pH variations at different time scales. Algal Res 28, 200–210.

Xu, X., Kim, J.Y., Oh, Y.R., Park, J.M., 2014. Production of biodiesel from carbon sources of macroalgae, *Laminaria japonica*. Bioresour. Technol. 169, 455–461.

Yang, J.Q., Kalhan, S.C., Hanson, R.W., 2009. What is the metabolic role of phosphoenolpyruvate carboxykinase? J. Biol. Chem. 284 (40), 27025–27027.

Ye, N.H., Zhang, X.W., Miao, M., et al., 2015. *Saccharina* genomes provide novel insight into kelp biology. Nat. Commun. 6, 6986.